

High-spin states in  $^{60}\text{Cu}$ 

Tsan Ung Chan, M. Agard,\* J. F. Bruandet, B. Chambon,<sup>†</sup> A. Dauchy, D. Drain,<sup>†</sup>  
A. Giorni, F. Glasser, and C. Morand

*Institut des Sciences Nucléaires, Université de Grenoble,  
38026 Grenoble Cédex, France*

(Received 25 January 1982; revised manuscript received 30 March 1982)

The  $^{60}\text{Cu}$  nucleus has been studied via the  $^{58}\text{Ni}(\alpha, pn\gamma)$  reaction using different techniques of in-beam  $\gamma$  spectroscopy. As in the other odd-odd Cu isotopes, the  $g_{9/2}$  shell plays an important role for the explanation of observed high-spin states. Some of these (particularly  $6^-$  and  $9^+$  states) could be interpreted as two-nucleon states in the framework of a crude shell model.

[ NUCLEAR REACTIONS  $^{58}\text{Ni}(\alpha, pn\gamma)$ ,  $E=24-40$  MeV; measured  
 $E_\gamma$ ,  $I_\gamma(\theta)$ ,  $\gamma\text{-}\gamma$  coincidence lifetimes by DSAM;  $^{60}\text{Cu}$  deduced high-spin  
levels,  $J$ ,  $\pi$ . ]

## I. INTRODUCTION

The  $(\alpha, d)$  (Ref. 1) and the  $(\alpha, ^2\text{He})$  (Ref. 2) reactions are known to be very selective. They populate preferentially two-nucleon high-spin states where the two transferred nucleons are coupled to their maximum spin value. We have deduced a very simple rule<sup>3</sup> from the crudest shell-model picture: The energy of such a two-nucleon state is simply equal to the sum of the two individual single-particle energies, plus a pairing energy when the two nucleons are identical. This simple calculation without any free parameter could account for a large number of experimental data involving two-nucleon states populated by the  $(\alpha, d)$  reaction or the  $(\alpha, ^2\text{He})$  reaction. Such states have often been observed and studied through fusion-evaporation reactions. The comparison of results from  $\gamma$  spectroscopy and transfer reactions was always fruitful in the Cu mass region.

All the information about  $^{60}\text{Cu}$  available until 1979 has been summarized by Auble.<sup>4</sup> Only a few levels of low excitation energy are well known. Recently, Zimmerman *et al.*<sup>5</sup> have determined many levels in  $^{60}\text{Cu}$  with a precision of  $\pm 10$  keV via the  $(^3\text{He}, t)$  reaction. However,  $J^\pi$  values are not unique. The  $\gamma$  decay scheme of  $^{60}\text{Cu}$  is deduced mainly from the radioactivity of  $^{60}\text{Zn}$  (Ref. 6) and from the  $^{60}\text{Ni}(p, n\gamma)^{60}\text{Cu}$  (Ref. 7) reaction.

II. EXPERIMENTAL PROCEDURES  
AND ANALYSIS OF DATA

Using beams from the Grenoble cyclotron, isotopic  $\sim 1$  mg/cm<sup>2</sup>  $^{58}\text{Ni}$  targets, and large volume

Ge(Li) detectors (50–90 cm<sup>3</sup>) with a typical resolution of 3 keV at  $E_\gamma=1.3$  MeV, the following measurements have been undertaken on the  $^{58}\text{Ni}(\alpha, pn\gamma)^{60}\text{Cu}$  reaction: the yield function of  $\gamma$  rays:  $E_\alpha=23-40$  MeV; the angular distributions at  $E_\alpha=32$  MeV performed at 8 angles from 30° to 150° on an isotopic target with Bi backing in order to reduce Doppler shifts; the  $\gamma\text{-}\gamma$  coincidences at  $E_\alpha=32$  MeV; the lifetime measurements with DSAM at  $E_\alpha=32$  MeV; and the lifetime measurements by electronic methods (lower limit  $\tau=3$  ns).

Figure 1 shows a single  $\gamma$ -ray spectrum of  $^{58}\text{Ni}+\alpha$  at  $E_\alpha=32$  MeV. The main channels are  $(\alpha, 2p\gamma)^{60}\text{Ni}$ ,  $(\alpha, pn\gamma)^{60}\text{Cu}$ , and  $(\alpha, \alpha p\gamma)^{57}\text{Co}$  with relative intensities of 6, 3, and 1. An accurate calibration of high energy gamma was provided by intense gamma rays from the radioactivity of  $^{60}\text{Cu}$  (in particular the following  $\gamma$  rays were used: 1332.5, 1791.6, 2158.9, and 3124.1 keV).

*Yield functions.* Figure 2 shows the relative intensity of some  $\gamma$  rays. As for other  $(\alpha, pn\gamma)$  reactions with Ni targets, the curves are rather flat except for  $\gamma$  issued from high-spin states.

*Angular distributions.* Yamazaki's formalism<sup>8</sup> was used to analyze the angular distribution measurements. The extracted  $A_2$  and  $A_4$  coefficients are listed in Table I. Generally, it is not possible to obtain a unique spin assignment from this measurement alone. However, we quote only the final adopted solution with regard to the coherence of the whole available information.

*$\gamma\text{-}\gamma$  coincidences.* An electronic timing measurement showed no isomeric levels with  $T_{1/2} > 2$  ns. Thus, prompt  $\gamma\text{-}\gamma$  coincidences were sufficient to establish the level scheme. The data were recorded

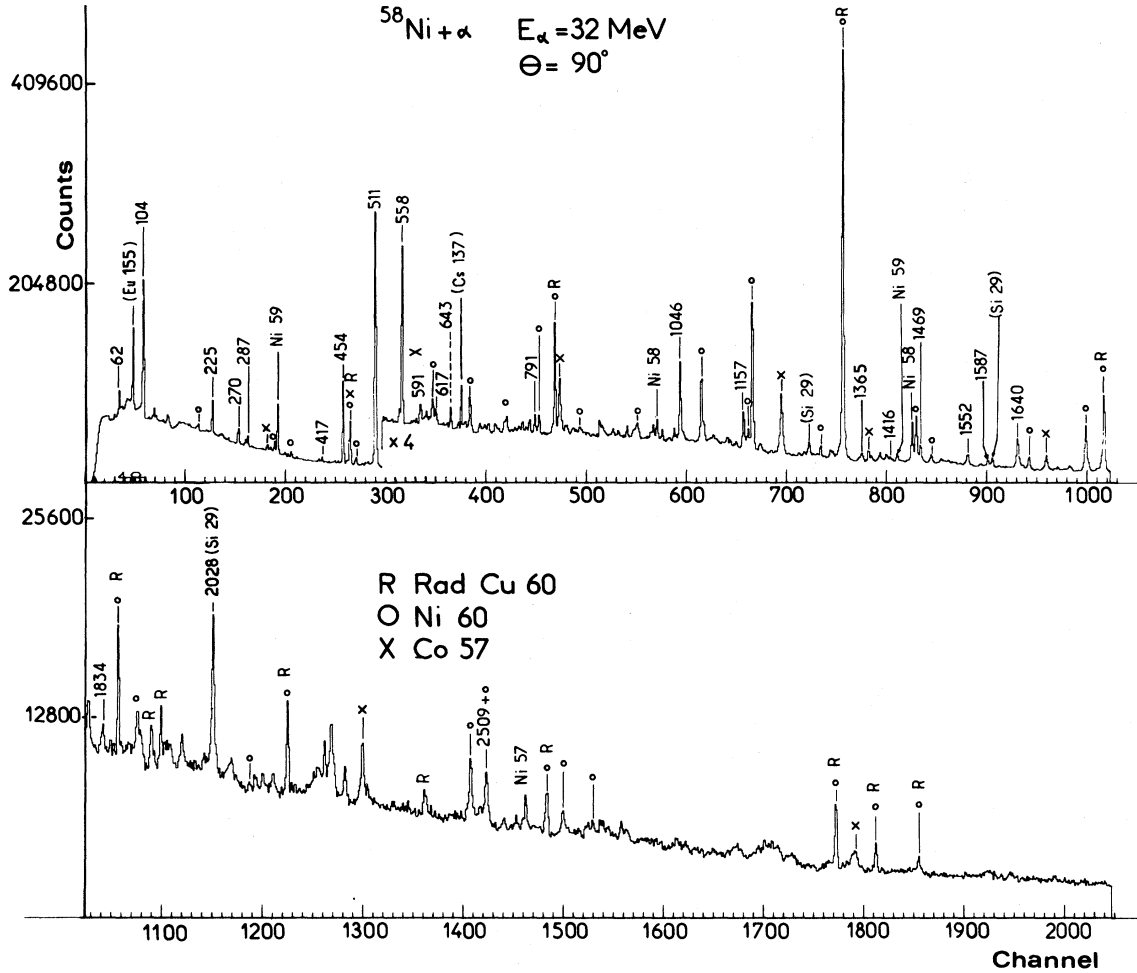


FIG. 1. Single spectra of the  $^{58}\text{Ni} + \alpha$  reaction at  $E_\alpha = 32$  MeV.

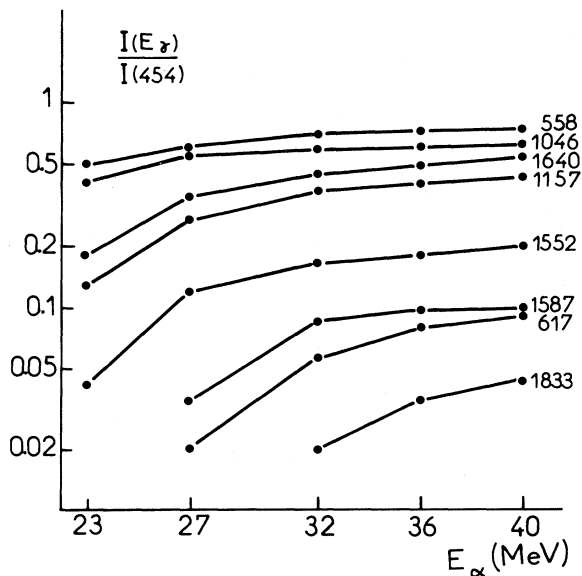


FIG. 2. Relative yield functions of some  $\gamma$  rays in  $^{60}\text{Cu}$ .

on magnetic tapes in the  $2048 \times 2048$  format [ $E_\gamma$  up to 2 MeV with one Ge(Li) and up to 4 MeV in the other Ge(Li)]. The two Ge(Li) detectors were perpendicular to the beam axis. The angle between them was  $90^\circ$  and they were separated by a thick sheet of Pb; thus the 511-511 keV coincidence from  $\beta^+$  decay of  $^{60}\text{Cu}$  and the backscattering from one detector to the other were strongly reduced. Figure 3 presents some selected spectra observed in coincidence with events in the indicated gate regions and with subtracted backgrounds. It may be noted that a few lines, such as 553, 591, and 643 keV, belong (at least partly) to  $^{60}\text{Cu}$  and must probably be located at the top of the level scheme. However, from  $\gamma$ - $\gamma$  coincidences and intensities in a single spectrum, they cannot be placed unambiguously. Moreover, some  $\gamma$  rays seen on the 558 keV gate are in fact in coincidence with the close perturbing 553 keV line.

*DSAM measurements.* We used a self-supporting

TABLE I. Results of the angular distribution measurements in  $^{60}\text{Cu}$ .  $E_\gamma$  transition decays from  $E_i$  state ( $J^\pi=J_i$ ) to  $E_f$  state ( $J^\pi=J_f$ ).  $A_2$  and  $A_4$  are coefficients of Legendre polynomials from  $I(\theta)=I_0 [1+A_2P_2(\cos\theta)+A_4P_4(\cos\theta)]$  and  $I_0(453.8)=100$ . The energies are in keV with a precision of 0.2 keV. The alignment parameters  $\alpha_2^i$  and  $\alpha_2^f$  of the initial and final levels are computed using a Gaussian substates distribution of width  $\sigma$  with formula and notations of Yamazaki.<sup>8</sup> The error on  $\alpha_2$  is typically 0.15.

$E_\gamma$	$E_i \rightarrow E_f$	$I_0$	$A_2 \pm \Delta A_2$	$A_4 \pm \Delta A_4$	$J_i \rightarrow J_f$	$\sigma$	$\alpha_2^i \rightarrow \alpha_2^f$	$\delta \pm \Delta \delta$	$\chi^2$	Multipolarity and remarks
62.3	62.3 $\rightarrow$ 0	14 $\pm$ 1	0.016 $\pm$ 0.12	-0.16 $\pm$ 0.17	1 <sup>+</sup> $\rightarrow$ 2 <sup>+</sup>	0.55	0.58 0.38	-0.17 $^{+1}_-$	0.9	/
103.7	557.5 $\rightarrow$ 453.8	50 $\pm$ 2	-0.24 $\pm$ 0.05	0.0 $\pm$ 0.08	4 <sup>+</sup> $\rightarrow$ 3 <sup>+</sup>	1.82	0.55 0.49	-0.03 $^{+0.5}_-$	0.75	M1
166.6	453.8 $\rightarrow$ 287.2	1.2 $\pm$ 0.2	-0.35 $\pm$ 0.14	0.12 $\pm$ 0.18	3 <sup>+</sup> $\rightarrow$ 2 <sup>+</sup>	1.53	0.49 0.38	-0.18 $^{+0.2}_-$	0.85	
224.9	287.2 $\rightarrow$ 62.3	23.7 $\pm$ 1	-0.20 $\pm$ 0.01	0.06 $\pm$ 0.02	2 <sup>+</sup> $\rightarrow$ 1 <sup>+</sup>	1.17	0.43 0.21	0 $^{+0.2}_-$	3.0	M1
270.3	557.5 $\rightarrow$ 287.2	17.8 $\pm$ 1	0.26 $\pm$ 0.02	-0.11 $\pm$ 0.03	4 <sup>+</sup> $\rightarrow$ 2 <sup>+</sup>	1.66	0.60 0.42	-0.07 $^{+0.1}_-$	0.74	E2
287.2	287.2 $\rightarrow$ 0	10.3 $\pm$ 0.5	0.02 $\pm$ 0.03	0.04 $\pm$ 0.04	2 <sup>+</sup> $\rightarrow$ 2 <sup>+</sup>	1.2	0.42 0.19	0.17 $^{+0.2}_-$	1.27	
327.2	781.0 $\rightarrow$ 453.8	4.0 $\pm$ 0.6	-0.03 $\pm$ 0.27	0.63 $\pm$ 0.26	3 <sup>+</sup> $\rightarrow$ 3 <sup>+</sup>					
357.0	914.5 $\rightarrow$ 557.5	2.0 $\pm$ 0.6	-0.22 $\pm$ 0.21	0.20 $\pm$ 0.30	3 <sup>+</sup> (4 <sup>+</sup> ) $\rightarrow$ 4 <sup>+</sup>					
417.5	3772.0 $\rightarrow$ 3354.5	5.9 $\pm$ 0.6	0.27 $\pm$ 0.10	0.20 $\pm$ 0.13	7 <sup>-</sup> $\rightarrow$ 7 <sup>-</sup>	2.2	0.74 0.69	-0.46 $^{+0.3}_-$	1.5	
453.8	453.8 $\rightarrow$ 0	100	-0.39 $\pm$ 0.03	0.07 $\pm$ 0.04	3 <sup>+</sup> $\rightarrow$ 2 <sup>+</sup>	1.53	0.49 0.38	-0.2 $^{+0.2}_-$	1.6	M1
460.7	914.5 $\rightarrow$ 453.8	4 $\pm$ 1.2	0.03 $\pm$ 0.25	0.40 $\pm$ 0.31	3 <sup>+</sup> (4 <sup>+</sup> ) $\rightarrow$ 3 <sup>+</sup>					
552.6		$\sim$ 4								
557.5	557.5 $\rightarrow$ 0	92.2 $\pm$ 2	0.23 $\pm$ 0.01	-0.04 $\pm$ 0.01	4 <sup>+</sup> $\rightarrow$ 2 <sup>+</sup>	2.1	0.49 0.38	0 $\pm$ 0.07	0.75	E2
616.5	3772.0 $\rightarrow$ 3155.5	6.6 $\pm$ 0.6	-0.34 $\pm$ 0.06	-0.01 $\pm$ 0.08	7 <sup>-</sup> $\rightarrow$ 6 <sup>-</sup>	1.79	0.80 0.77	-0.05 $^{+0.1}_-$	0.76	
642.9		$\sim$ 4								
781.0	781.0 $\rightarrow$ 0	5.0 $\pm$ 0.5	-1.09 $\pm$ 0.12	0.17 $\pm$ 0.14	3 <sup>+</sup> $\rightarrow$ 2 <sup>+</sup>	0.7	0.88 0.48	-0.7 $^{+0.5}_-$	0.8	M1/E2
790.5	2817.1 $\rightarrow$ 2026.6	8.2 $\pm$ 0.5	-0.32 $\pm$ 0.4	0.04 $\pm$ 0.28	(6) $\rightarrow$ 5 <sup>+</sup>	1.5	0.84 0.80	0.00 $^{+0.6}_-$	0.8	

TABLE I. (Continued.)

$E_\gamma$	$E_i \rightarrow E_f$	$I_0$	$A_2 \pm \Delta A_2$	$A_4 \pm \Delta A_4$	$J_i \rightarrow J_f$	$\sigma$	$\alpha_2^i \rightarrow \alpha_2^f$	$\delta \pm \Delta \delta$	$\chi^2$	Multipolarity and remarks
967.7	1421.5 $\rightarrow$ 453.8	5.0 $\pm$ 0.5			3 <sup>+</sup> (4 <sup>+</sup> ) $\rightarrow$ 3 <sup>+</sup>					perturbed by other lines
1046.1	1603.6 $\rightarrow$ 557.5	42.8 $\pm$ 2	-0.95 $\pm$ 0.01	0.13 $\pm$ 0.01	5 <sup>+</sup> $\rightarrow$ 4 <sup>+</sup>	1.52	0.77 0.64	-0.9 $\pm$ 0.1	0.79	M1/E2
1088.1	2691.7 $\rightarrow$ 1603.6	6.7 $\pm$ 1	-1.57 $\pm$ 0.38	0.0 $\pm$ 0.22	6 <sup>+</sup> $\rightarrow$ 5 <sup>+</sup>	1.50	0.84 0.72	-1.2 $^{+0.5}_{-0.5}$	5.0	M1/E2
1157.3	3354.5 $\rightarrow$ 2197.2	30.4 $\pm$ 1.5	-0.29 $\pm$ 0.04	0.17 $\pm$ 0.05	7 <sup>-</sup> $\rightarrow$ 6 <sup>+</sup>	2.06	0.77 0.74	-0.03 $^{+0.1}_{-0.1}$	2.8	
1166.3	4520.8 $\rightarrow$ 3354.5									perturbed by $\gamma$ in $^{60}\text{Ni}$
1221.4	1778.9 $\rightarrow$ 557.5				5 <sup>+</sup> $\rightarrow$ 4 <sup>+</sup>					perturbed by $\gamma$ in $^{57}\text{Co}$
1325.1	1778.9 $\rightarrow$ 453.8	10.7 $\pm$ 1	0.50 $\pm$ 0.04	-0.09 $\pm$ 0.06	5 <sup>+</sup> $\rightarrow$ 3 <sup>+</sup>	1.2	0.86 0.71	-0.09 $^{+0.2}_{-0.2}$	0.8	E2
1365.3	4520.8 $\rightarrow$ 3155.5									perturbed by $\gamma$ in $^{61}\text{Cu}$ and $^{59}\text{Ni}$
1416.1	5188.1 $\rightarrow$ 3772.0	3.8 $\pm$ 0.4	0.09 $\pm$ 0.12	0.31 $\pm$ 0.20	9 <sup>-</sup> $\rightarrow$ 7 <sup>-</sup>	2.18	0.84 0.80	-0.18 $\pm$ 0.2	0.90	
1469.1	2026.6 $\rightarrow$ 557.5	14.8 $\pm$ 1.5	-0.80 $\pm$ 0.09	0.20 $\pm$ 0.11	5 <sup>+</sup> $\rightarrow$ 4 <sup>+</sup>	1.45	0.79 0.60	-1.7 $^{+0.8}_{-0.5}$	0.8	M1/E2
1551.9	3155.5 $\rightarrow$ 1603.6	16 $\pm$ 1.5	-0.42 $\pm$ 0.04	0.19 $\pm$ 0.06	6 <sup>-</sup> $\rightarrow$ 5 <sup>+</sup>	1.8	0.77 0.73	-0.1 $^{+0.2}_{-0.4}$	2.4	E1
1587.2	3190.8 $\rightarrow$ 1603.6	7.7 $\pm$ 0.7	0.31 $\pm$ 0.10	0.22 $\pm$ 0.12	7 <sup>+</sup> $\rightarrow$ 5 <sup>+</sup>	2.5	0.67 0.62	-0.03 $^{+0.3}_{-0.3}$	2.3	E2
1639.7	2197.2 $\rightarrow$ 557.5	56.8 $\pm$ 3	0.33 $\pm$ 0.06	-0.23 $\pm$ 0.11	6 <sup>+</sup> $\rightarrow$ 4 <sup>+</sup>	1.45	0.85 0.76	0.0 $\pm$ 0.15	0.98	E2
1792.0	2349.5 $\rightarrow$ 557.5									perturbed by $\gamma$ in $^{60}\text{Ni}$
1833.6	5188.1 $\rightarrow$ 3354.5	3.2 $\pm$ 0.5	0.22 $\pm$ 0.07	-0.06 $\pm$ 0.11	9 <sup>-</sup> $\rightarrow$ 7 <sup>-</sup>	2.75	0.75 0.71	-0.14 $^{+0.1}_{-0.2}$	0.98	E2
2509.0	3066.5 $\rightarrow$ 557.5				(5) $\rightarrow$ 4 <sup>+</sup>					perturbed by $\gamma$ in $^{60}\text{Ni}$

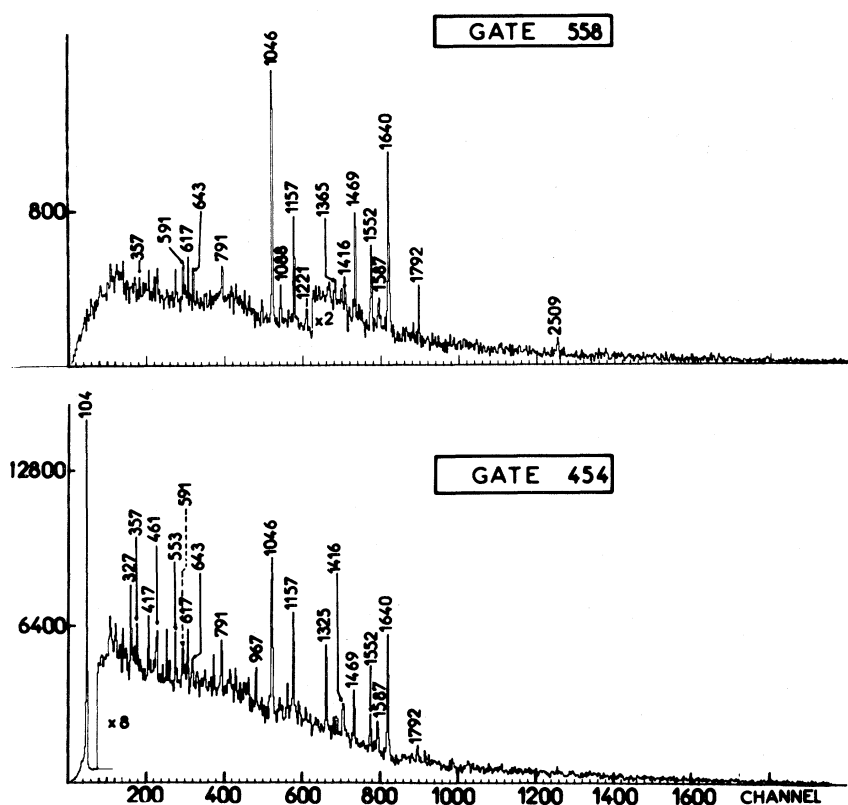


FIG. 3. Selected spectra in coincidence with events in the indicated regions and with subtracted background.

0.9 mg/cm<sup>2</sup> thick <sup>58</sup>Ni target following the method described at length in Ref. 9. A long lifetime  $\gamma$  transition is used; here, the 1084 keV transition in <sup>60</sup>Ni with a lifetime of  $\tau=423\pm 70$  ps according to the work of Moyat *et al.*<sup>10</sup> to determine the nuclear stopping power which is assumed to show the following pattern:  $d\epsilon/d\rho=ax/\exp(x^2/2)$  with  $x=b\epsilon^{1/2}$ . The values of  $a$  and  $b$  are  $a=1.08$ ,  $b=1.1$ . All the lifetimes were found to be longer than 4 ps except those given in Table II. [We give results only for the shortest ones when the Doppler-shift attenuation method (DSAM) can be reliably applied.] Typical fits are shown in Fig. 4.

**Spin parity assignments.** Spin-parity assignments were deduced with more or less reliability using the following:

(i) the fact that in the fusion evaporation reactions, strongly populated  $\gamma$  cascades usually proceed from higher to lower spins;

(ii) the angular distribution measurements (see Table I). For two  $\gamma$  rays,  $\gamma_1$  and  $\gamma_2$  ( $\gamma_1$  feeding the level and  $\gamma_2$  emanating from the level) the  $\alpha_2^f(\gamma_1)$  value of the alignment parameter for the level calculated by the  $\gamma_1$  angular distribution analysis should be near  $\alpha_2^f(\gamma)$ , the value calculated for the

same level by the  $\gamma_2$  angular distribution analysis;

(iii) the yield functions—increasing slope corresponds to increasing spin;

(iv) the lifetime measurements or estimations (see Table II). As all the transitions have  $T_{1/2}<2$  ns, quadrupolar  $\gamma$  rays with  $E_\gamma<1300$  keV have  $E2$  multipolarity (any  $M2$  with  $E_\gamma<1300$  keV would have an observable lifetime by the electronic method); and

(v) the  $(\alpha,d)$  reaction results.<sup>1,11</sup> In particular,  $J=6$  and 7 states strongly populated in this reaction are two-nucleon states and thus should have negative parity.

The deduced level scheme is shown in Fig. 5. Table III presents the branching ratios of some levels in <sup>60</sup>Cu.

**The 287.2 keV level.** Auble<sup>4</sup> adopts  $J^\pi=(1^+,2^+)$ .  $J^\pi=1^+$  must be rejected because this level is fed by a 270 keV  $\gamma$  ray ( $E2$  transition) from the 557.5 keV level with  $J^\pi=4^+$  (see below).

**The 453.8 keV level.** This level observed in the (<sup>3</sup>He, $t$ ) reaction<sup>5</sup> with  $l=4$  has positive parity ( $J^\pi=3^+, 4^+, 5^+$ ) decays through an  $M1$  transition to the ground state ( $J^\pi=2^+$ ). Another weak branch (about 1%) of 167 keV  $\gamma$  is observed. Therefore,

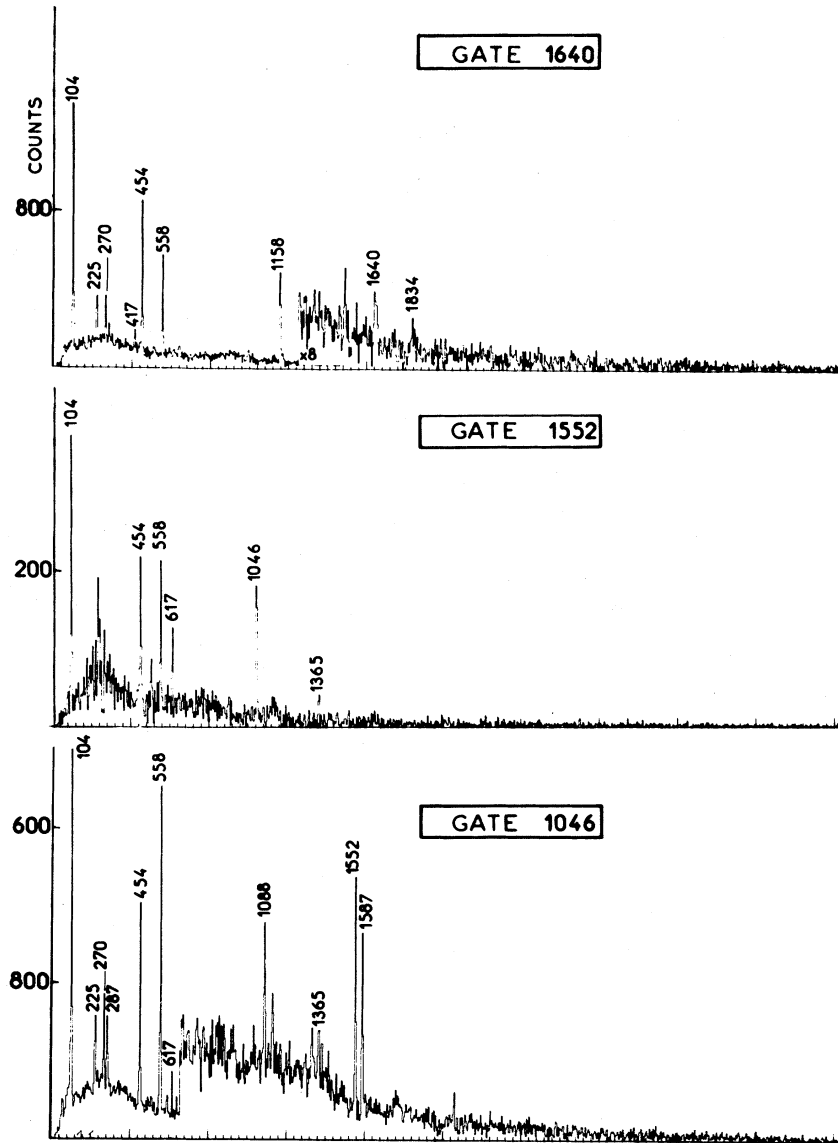


FIG. 3. (Continued.)

TABLE II. Lifetime measurements.  $E_x$  and  $J^\pi$  are, respectively, the excitation energy and the characteristics of the studied level which decays through a  $\gamma$  line of  $E_\gamma$  energy.  $\tau_i$  is the deduced lifetime at the angle  $\theta_i^0$  degrees,  $\tau_j$  is the final adopted value. Central values  $\tau_i$  and  $\tau_j$  are flanked by the lower  $\tau_L$  and upper  $\tau_U$  limits. Crosses indicate the electronic measurements upper limit. Energies are expressed in keV, lifetimes in ps, and  $\gamma$  strengths in Weisskopf units.

$E_x$	$J^\pi$	$E_\gamma$	$\theta_i^0$	$\tau_L < \tau_i < \tau_U$	$\tau_L < \tau_j < \tau_U$	$ M ^2$ W.u.	
						$E_1$	$E_2$
2197	$6^+$	1640	25	$0.6 < 1 < 2.6$	$0.7 < 1.6 < 5$		3
			160	$0.8 < 2.6 < 10$			
3156	$6^-$	1552	25	$1 < 2.4 < \infty$	$1 < 5 < 3000^+$	$3.10^{-5}$	
			160	$1 < 10 < \infty$			
3191	$7^+$	1587	160	$1 < 2.4 < \infty$	$1 < 2.4 < 3000^+$		2.5
5188	$9^-$	1834	25	$0.6 < 1.2 < 8$	$0.7 < 1.5 < 10$		1
			160	$0.8 < 2 < \infty$			

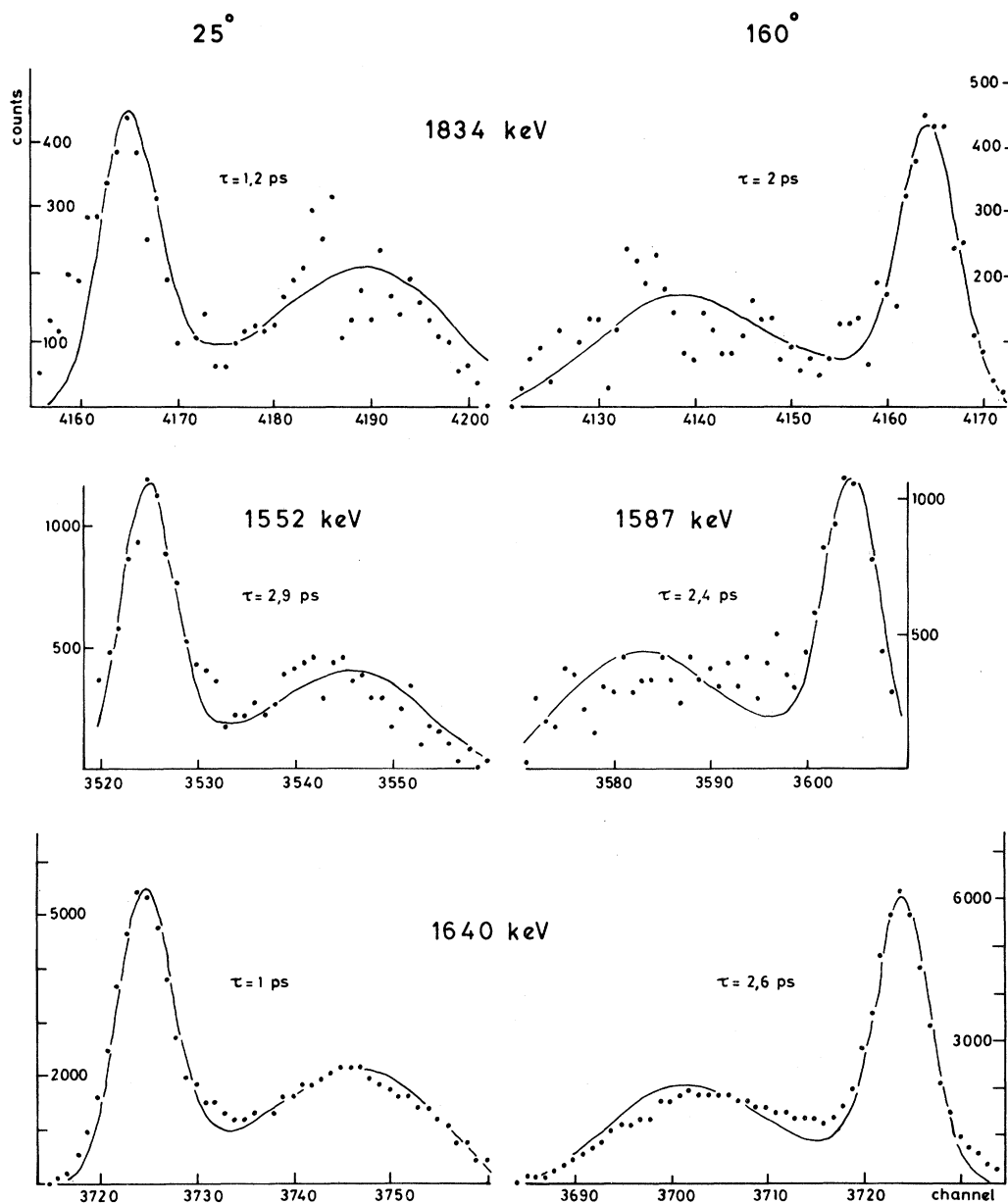


FIG. 4. Line shape fits with DSAM calculations for some  $\gamma$  rays of  $^{60}\text{Cu}$  in singles spectra at forward and backward angles with  $E_{\alpha}=32$  MeV.

the characteristics are  $J^{\pi}=3^{+}$ .

*The 557.5 keV level.* The characteristics  $J^{\pi}=4^{+}$  are confirmed by angular distributions of three  $\gamma$  rays issued from this level: 558 keV ( $E2$ ), 270 keV ( $E2$ ), and 104 keV ( $M1$ ). An  $E2$  character is assigned by lifetime considerations as mentioned above.

*The 781.0 keV level.* Two  $\gamma$  are issued from this state. The  $(^3\text{He}, t)$  reaction attributes  $3^{+}(4^{+})$  to this level. The characteristics  $J^{\pi}=3^{+}$  are adopted since

the 781 keV  $\gamma$  ray is an  $M1/E2$  transition ( $3^{+}\rightarrow 2^{+}$  g.s.).

*The 914.5 keV level.* This state may be identified with the 900 keV one observed via  $(^3\text{He}, t)$ . Its  $\gamma$  decay is compatible with the previous assignments  $J^{\pi}=3^{+}, (4^{+})$ . The angular distribution of the weak 358 keV line favors  $J^{\pi}=3^{+}$  ( $A_2 < 0$ ).

*The 1421.5 keV level.* It can be identified with the 1432 keV state seen in the  $(^3\text{He}, t)$  reaction, but the angular distribution of the 967 keV  $\gamma$  ray cannot

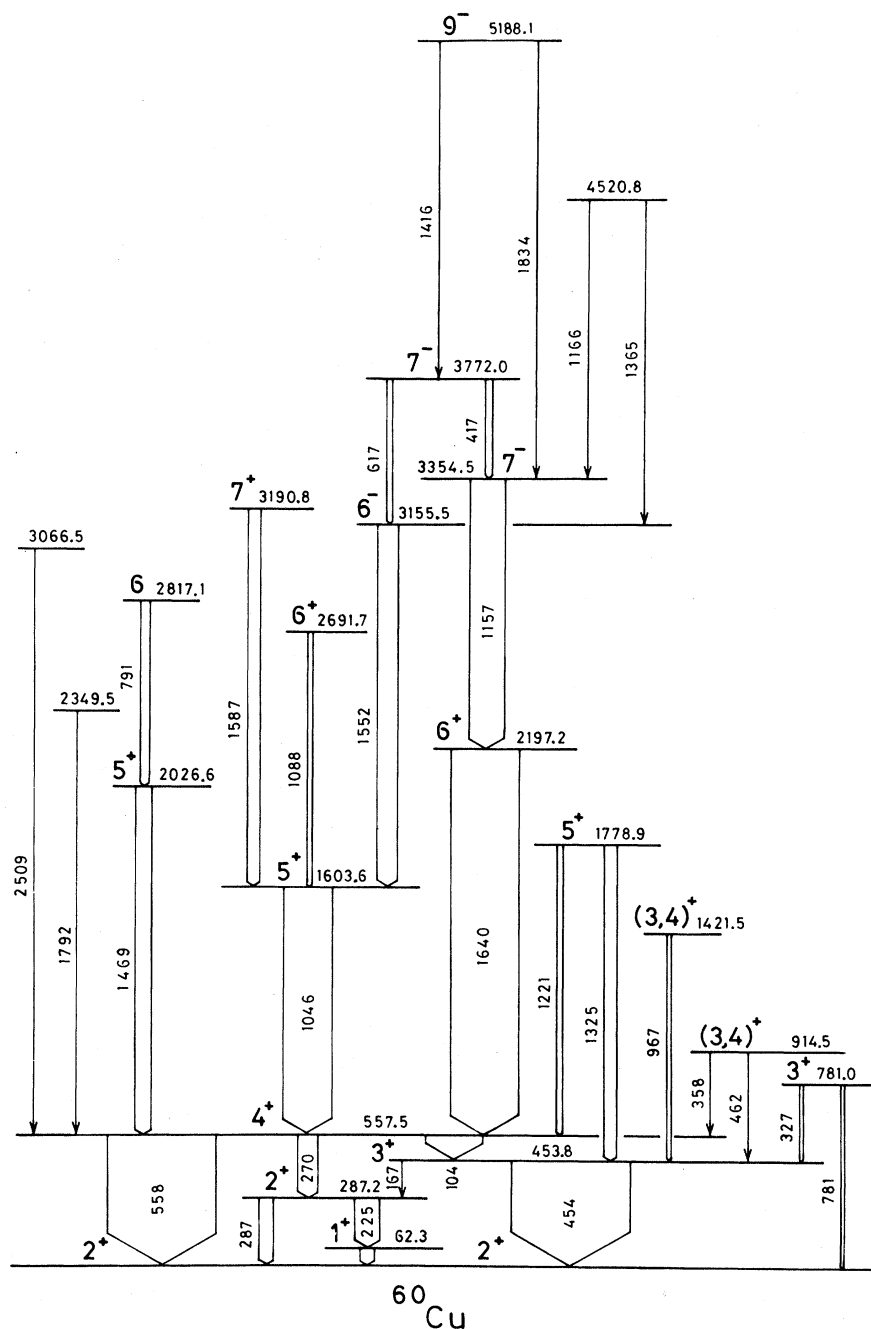


FIG. 5. Decay scheme of  $^{60}\text{Cu}$  as a result of the present measurements.

rule out one of the proposed  $J^\pi = (3^+, 4^+)$ .

*The 1603.6 keV level.* It decays to the 557.5 keV level ( $J^\pi = 4^+$ ) by an  $M1/E2$ , 1046 keV  $\gamma$  ray. Therefore, this level has  $J^\pi = 5^+$ . It is strongly populated in the  $(^3\text{He}, t)$  reaction with  $l=6$  ( $J^\pi = 5^+, 6^+$ ) and in the  $(\alpha, d)$  reaction which favors two-nucleon states. We conclude from the above arguments that it is very probably the

$(\pi f_{5/2} \nu f_{5/2})_{5^+}$  state.

*The 1778.9 keV level.* This new level decays by two transitions: a 1325 keV  $E2$  transition to the  $3^+$  state at 453.8 keV and 1221 keV  $\gamma$  ray perturbed by the 1224 keV  $\gamma$  ray in  $^{57}\text{Co}$ . Therefore, this level has the characteristics of a  $J^\pi = 5^+$  state.

*The 2026.6 keV level.* A 1469 keV  $M1/E2$  transition ( $A_2 = -0.8$ ,  $\delta = 1.7$ ) originating from this



TABLE III. Branching ratios of some levels in  $^{60}\text{Cu}$ .

Levels	$J^\pi$	$E_i \rightarrow E_f$	$E_\gamma$	Branching ratios %
287	$2^+$	287 $\rightarrow$ 0	287	$30 \pm 3$
		287 $\rightarrow$ 62	225	$70 \pm 3$
454	$3^+$	454 $\rightarrow$ 0	454	$99 \pm 0.5$
		454 $\rightarrow$ 287	167	$1 \pm 0.5$
558	$4^+$	558 $\rightarrow$ 0	558	$58 \pm 4$
		558 $\rightarrow$ 287	270	$11 \pm 1$
		558 $\rightarrow$ 454	104	$31 \pm 3$
781	$3^+$	781 $\rightarrow$ 0	781	$55 \pm 6$
		781 $\rightarrow$ 454	327	$45 \pm 6$
914	$3^+(4^+)$	914 $\rightarrow$ 454	462	$67 \pm 15$
		914 $\rightarrow$ 558	357	$33 \pm 15$
3772	$7^-$	3772 $\rightarrow$ 3155	617	$53 \pm 5$
		3772 $\rightarrow$ 3355	417	$47 \pm 5$
5188	$9^-$	5188 $\rightarrow$ 3772	1416	$54 \pm 7$
		5188 $\rightarrow$ 3355	1834	$46 \pm 7$

new state feeds the  $J^\pi=4^+$  level. We, therefore, assign  $J^\pi=5^+$  to this level.

*The 2197.2 keV level.* This state is strongly populated via  $(\alpha, pn\gamma)$  and decays by a 1640 keV  $E2$  transition ( $L=2$  from angular distribution and  $\tau=2$  ps) with an increasing yield function. It is proposed as the  $6^+$  yrast level. (However, we notice that the 1640 keV  $\gamma$  ray is not unique. It is in coincidence with another  $\simeq 1640$  keV  $\gamma$  ray, but it can be estimated from coincidence measurements that the intensity of the second 1640 keV  $\gamma$  ray represents only 10% of the whole.)

*The 2349.5 keV level.* This new level decays by a 1792 keV  $\gamma$  ray. Spin assignment is not possible because of an intense 1792 keV  $\gamma$  ray in  $^{60}\text{Ni}$ .

*The 2691.7 keV level.* The 1088 keV  $\gamma$  ray has  $M1/E2$  behavior and thus implies  $J^\pi=6^+$  for this new level.

*The 2817.1 keV level.* The angular distribution measurements imply  $L=1$  to the 791 keV  $\gamma$  ray and therefore suggest spin 6 for this new state.

*The 3066.5 keV level.* This level is deexcited by a 2509 keV  $\gamma$  ray (see gate 558). Unfortunately, another  $\gamma$  ray with about the same energy belongs to  $^{60}\text{Ni}$  with comparable intensity, so it is hazardous to give any spin assignment.

*The 3155.5 keV level.* This state decays through a 1552 keV  $L=1$  transition. Its increasing yield function suggests  $J=6$  for this state. Now, using

the  $^{58}\text{Ni}(\alpha, d)^{60}\text{Cu}$  reaction, Lu *et al.*<sup>1</sup> have observed a strongly excited doublet at 3.29 MeV using 50 MeV  $\alpha$  projectiles and Sanderson *et al.*<sup>10</sup> have shown with  $E_\alpha=26$  MeV that the two components of the doublet are located at 3.15 and 3.33 MeV. So the 3155.5 keV level can be identified with the 3.15 MeV state seen in  $(\alpha, d)$ , which assigns negative parity and thus the  $J^\pi=6^-$  characteristics to this level.

*The 3190.8 keV level.* The 1587 keV  $\gamma$  ray is an  $E2$  transition ( $L=2$  from angular distribution, and a lifetime of 3 ps rules out the  $M2$  character). With regard to the increasing yield function, a  $J^\pi=7^+$  assignment is quite certain.

*The 3354.5 keV level.* An intense 1157 keV  $L=1$  transition deexcites this level. Its yield increases with increasing  $E_\alpha$ . This state can be identified with the 3.33 MeV level strongly excited in the  $(\alpha, d)$  reaction. This confers  $J^\pi=7^-$  to this state.

*The 3772.0 keV level.* This state is deexcited by two  $\gamma$  transitions of about the same intensity. The 617 keV  $\gamma$  ray has  $L=1$  character while the 417 keV  $\gamma$  ray has  $A_2 \simeq 0.26$ , compatible with a  $J \rightarrow J$  transition. We assign  $J=7$  and negative parity to this level since it is strongly excited in the  $(\alpha, d)$  reaction.<sup>1,10</sup>

*The 4520.8 keV level.* Two perturbed  $\gamma$  rays deexcite this state; consequently no spin can be assigned.

*The 5188.1 keV level.* Two  $L=2$  transitions originate from this level. An  $E2$  character is assigned to the 1834 keV  $\gamma$  ray because the lifetime of the initial state is 2 ps. The rapidly increasing yield function favors a  $9^-$  assignment. The  $(\pi g_{9/2}, \nu g_{9/2})_{9^+}$  level seen via  $(\alpha, d)$  at 5.99 MeV was not sufficiently populated to make the observation of its  $\gamma$  decay possible.

### III. DISCUSSION

As a first approximation  $^{60}\text{Cu}$  can be regarded as a  $^{56}\text{Ni}$  inert core plus one proton and three neutrons in other active shells. When the four valence particles are restricted only to the  $p_{3/2}$ ,  $p_{1/2}$ , and  $f_{5/2}$  orbits, as in the calculations of Koops *et al.*<sup>12</sup> and Wang *et al.*,<sup>13</sup> the highest allowed spin is  $J^\pi=8$ . Energy and electromagnetic properties of levels with  $J^\pi=5^+$ ,  $6^+$ , and  $7^+$ , measured in this experiment, are in good agreement (see Table IV) with shell model calculations<sup>11</sup> performed either with MSDI (modified surface delta interaction) or ASDI (adjusted surface delta interaction). But to account for negative parity states or positive parity states

TABLE IV. Comparison between shell model calculations (Ref. 11) and experimental results for  $5^+$ ,  $6^+$ , and  $7^+$  levels in  $^{60}\text{Cu}$ .

$J_i^\pi$	Excitation energies			$J_f^\pi$	exp	Decay properties $ M ^2$ W.u.				
	exp	MSDI	ASDI			M1 MSDI	ASDI	exp	E2 MSDI	ASDI
$5^+$	1.604	1.76	1.69	$4^+$	$<4.10^{-3}$	0.069	0.039	$<5$	2.8	6.2
$5^+$	1.779 <sup>a</sup>	2.30	2.06							
$6^+$	2.197	2.40	2.03	$4^+$				3	11	11
	2.691 <sup>b</sup>	3.01	3.09							
$7^+$	3.191	3.27	3.01	$5^+$				2.5	11	11

<sup>a</sup>This level may have  $(\pi f_{7/2}^{-1}, \nu f_{5/2})_{5^+}$  configuration. The level calculated by Koops *et al.* (Ref. 11) may then be the 2.027 MeV level.

<sup>b</sup>This level may have  $(\pi f_{7/2}^{-1}, \nu f_{5/2})_{6^+}$  configuration.

with spin  $J > 8$  it is necessary to introduce the  $g_{9/2}$  shell (and/or the breaking of the  $^{56}\text{Ni}$  core).

The level scheme of  $^{60}\text{Cu}$  is quite similar to that of  $^{62}\text{Cu}$  (Ref. 14). The 3.155 MeV state  $J^\pi = 6^-$  decays via an  $E1$  transition to a  $5^+$  state which has mainly the configuration  $\pi f_{5/2}, \nu f_{5/2}$ . This behavior is different from that of  $^{64}\text{Cu}$  (Ref. 15) and  $^{66}\text{Cu}$  (Refs. 16 and 17) where the  $6^-$  level is isomeric and decays to a  $J^\pi = 4^+$  state through a  $M2$  transition.

This difference may be understood simply in the framework of our crude shell model<sup>3</sup> for two-nucleon states. Indeed, our addition rule predicts the excitation energy of the  $(\pi f_{5/2}, \nu f_{5/2})_{5^+}$  states in odd-odd Cu nuclei between 1 and 1.3 MeV, while the excitation energy of the  $(\pi p_{3/2}, \nu g_{9/2})_{6^-}$  states varies quickly from 1 MeV for  $^{66}\text{Cu}$  to 3 MeV for  $^{60}\text{Cu}$ . In the case of  $^{64}\text{Cu}$  and  $^{66}\text{Cu}$ , the  $5^+$  state may be very near the  $6^-$  level so it may explain why the  $6^- \rightarrow 5^+$  transition is not seen. In  $^{64}\text{Cu}$ , the lev-

el at 1.59 MeV may be double and one member of the doublet is the  $6^-$  state, the other may be the  $5^+$  state seen in  $(d, \alpha)$  reaction.<sup>16</sup> On the other hand, in  $^{62}\text{Cu}$  and  $^{60}\text{Cu}$ , the  $6^-$  state lies well above the  $5^+$  state and an intense  $6^- \rightarrow 5^+$   $E1$  transition is observed.

The  $6^-$  level is very strongly populated by the  $(\alpha, pn\gamma)$  reaction in all the studied odd-odd Cu nuclei ( $^{60}\text{Cu}$ ,  $^{62}\text{Cu}$ ,  $^{64}\text{Cu}$ ,  $^{66}\text{Cu}$ ). The  $9^+$  state is much less fed and in  $^{62}\text{Cu}$  and  $^{64}\text{Cu}$ ; it decays via an  $E1$  transition to the  $8^-$  state. Figure 6 shows the striking correlation between the excitation energies of the  $6^-$  and  $9^+$  states and the  $g_{9/2}$  single particle energies in odd-odd Cu nuclei. (Data for  $^{66}\text{Cu}$  and  $^{68}\text{Cu}$  are from Refs. 16–18.) For  $^{64}\text{Cu}$  and  $^{66}\text{Cu}$ , the  $(d, p)$  reactions give unambiguously the main configuration of the  $6^-$  state as  $(\pi p_{3/2}, \nu g_{9/2})_{6^-}$ . For  $^{60}\text{Cu}$  and  $^{62}\text{Cu}$ , the other configuration  $(\pi g_{9/2}, \nu p_{3/2})_{6^-}$  is also possible. In  $^{60}\text{Cu}$  our addition rule predicts neighboring energies for these two configurations:  $(\pi p_{3/2}, \nu g_{9/2})_{6^-}$  at 3.062 MeV and  $(\pi g_{9/2}, \nu p_{3/2})_{6^-}$  at 3.042 MeV. There is probably a mixing of these two configurations.

The confrontation of results from  $\gamma$  spectroscopy studies and transfer reactions has proven fruitful once more: The assignment of negative parity to the two observed  $J=7$  states is expected from the selection rule of the  $(\alpha, d)$  reaction and the main configuration can be assigned. As for the other Cu isotopes (and also for Zn, Ga, and Ge isotopes) we point out the importance of the role of the  $g_{9/2}$  shell to build high-spin states. It would be interesting if conventional shell-model calculations in this region of the chart of nuclides could include the  $g_{9/2}$  shell and afford in this way a deeper explanation of high-spin states.

The authors thank S. Schacke for a careful reading of the manuscript.

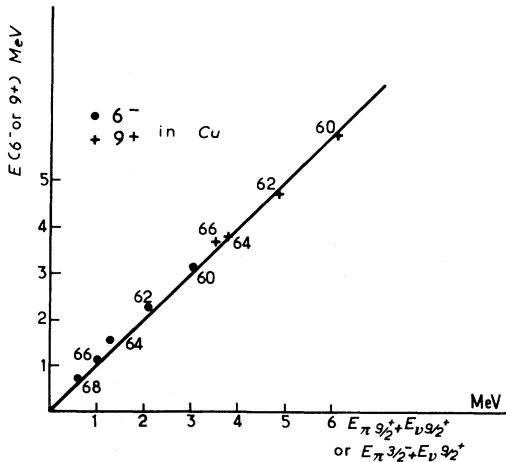


FIG. 6. Experimental energy of the  $J^\pi = 6^-$  and  $9^+$  states in odd-odd Cu isotopes as a function of the sum of two single particle energies.

- \*Permanent address: Institut des Sciences Exactes, Université de Constantine, Route d'Ain El Bey, Constantine, Algérie.
- †Permanent address: Institut de Physique Nucléaire (UCB Lyon, IN2P3), 43 Bd du 11 Novembre, 69621 Villeurbanne, France.
- <sup>1</sup>C. C. Lu, M. S. Zisman, and B. G. Harvey, *Phys. Rev.* **186**, 1086 (1969).
- <sup>2</sup>R. Jahn, D. P. Stahel, G. J. Wozniak, R. J. de Meijer, and J. Cerny, *Phys. Rev. C* **18**, 9 (1978).
- <sup>3</sup>Tsan Ung Chan, M. Agard, J. F. Bruandet, and C. Morand, *Phys. Rev. C* **19**, 244 (1979).
- <sup>4</sup>R. L. Auble, *Nucl. Data Sheets* **28**, 103 (1979).
- <sup>5</sup>W. R. Zimmerman, J. J. Kraushaar, M. J. Schneider, and H. Rudolph, *Nucl. Phys.* **A297**, 416 (1978).
- <sup>6</sup>G. H. Dulfer, B. O. ten Brink, T. J. Ketel, A. W. B. Kalshoven, and H. Verheul, *Z. Phys.* **251**, 416 (1972).
- <sup>7</sup>L. Birstein, Ch. Drory, A. A. Jaffe, and Y. Zioni, *Nucl. Phys.* **A97**, 203 (1967).
- <sup>8</sup>T. Yamazaki, *Nucl. Data* **A3**, 1 (1967).
- <sup>9</sup>C. Morand and Tsan Ung Chan, *Comput. Phys. Commun.* **23**, 393 (1981).
- <sup>10</sup>C. Moyat, B. Delaunay, J. Delaunay, J. Eberth, V. Zobel, and L. Cleemann, *Nucl. Phys.* **A318**, 236 (1979).
- <sup>11</sup>N. E. Sanderson, R. G. Summers Gill, T. Taylor, and A. Khan, Annual Report, Birmingham, 1976 (unpublished).
- <sup>12</sup>J. E. Koops and P. W. Glaudemans, *Z. Phys. A* **280**, 181 (1977).
- <sup>13</sup>M. C. Wang, H. C. Chiang, S. T. Hsieh, and E. K. Lin, *Nuovo Cimento* **29A**, 49 (1975).
- <sup>14</sup>Tsan Ung Chan, M. Agard, J. F. Bruandet, A. Giorni, F. Glasser, J. P. Longequeue, and C. Morand, *Nucl. Phys.* **A293**, 207 (1977).
- <sup>15</sup>Tsan Ung Chan, M. Agard, J. F. Bruandet, A. Giorni, and J. P. Longequeue, *Nucl. Phys.* **A257**, 413 (1976).
- <sup>16</sup>Y. S. Park and W. W. Daehnick, *Phys. Rev.* **180**, 1082 (1969).
- <sup>17</sup>Tsan Ung Chan, J. F. Bruandet, B. Chambon, A. Dauchy, D. Drain, A. Giorni, F. Glasser, and C. Morand, Proceedings of the International Conference on Nuclear Behavior at High Angular Momentum, Strasbourg, 1980 (unpublished).
- <sup>18</sup>R. L. Auble, *Nucl. Data Sheets* **14**, 155 (1975).